ORIGINAL RESEARCH

Grafting of multiwalled carbon nanotubes with pyrazole derivatives: characterization, antimicrobial activity and molecular docking study

Nadia Hanafy Metwally[1]
Gamal Riad Saad[1]
Esraa Azmy Abd El-Wahab[2]

[1]Chemistry Department, Faculty of Science, Cairo University, Giza, Egypt; [2]Department of Engineering Mathematics and Physics, Faculty of Engineering Shoubra, Benha University

Introduction: It is well known that the grafted multiwalled carbon nanotubes (MWCNTs) have antibacterial activity and lower cytotoxicity. Moreover, pyrazole derivatives have a broad spectrum of biological activity due to their fertile template for many medicinal drugs. On view of these findings we report herein the hybridization between MWCNTs and some pyrazole derivatives as antibacterial agents.

Materials and methods: Pyrazole and pyrazolone derivatives were grafted onto the surface of carboxylated MWCNTs via the reaction of carboxylated MWCNTs and the diazonium salts of pyrazoles and pyrazolones using mixed acid treatment. The insertion of the pyrazole and pyrazolone moieties was characterized by Fourier transform infrared (FTIR) spectroscopy, energy dispersion spectroscopy, transmission electron microscopy, X-ray diffraction and thermogravimetric (TGA).

Results: The results indicate that pyrazole and pyrazolone moieties successfully attached on carboxylated MWCNTs surface. The neat pyrazole and pyrazolone derivatives and their corresponding carbon nanotubes were tested against *Staphylococcus aureus, Bacillus subtilus, Escherichia coli*, and *Candida albicans* bacteria, and *Aspergillusniger* fungi. The results showed that the grafted carbon nanotubes of pyrazole and pyrazolone derivatives have better antimicrobial activity than the neat pyrazole and pyrazolone derivatives. The molecular docking studies were performed on the most potent antimicrobial compounds to investigate the existence of the interactions between the most active inhibitors and Farnesyl pyrophosphate synthase (FPPS).

Conclusion: The surface of the carboxylated MWCNTs was successfully grafted with some pyrazole derivatives. The antibacterial activity was investigated for the newly synthesized compounds and indicated that the grafted MWCNTs have good antibacterial activity toward some pathogenic types of bacteria.

Keywords: carbon nanotubes, pyrazoles, pyrazolones, grafting, antimicrobial activity, zeta-potential, molecular docking study

Correspondence: Nadia Hanafy Metwally
Chemistry Department, Faculty of Science, Cairo University, Giza 12613, Egypt
Email nhmmohamed@yahoo.com

Introduction

Recently, carbon nanotubes (CNTs) and their based materials have gained considerable attention due to their unique physical properties and potential for numerous biological applications.[1–4] Both single-walled and multi-walled carbon nanotubes (MWCNTs) have been found to possess antimicrobial activity.[5,6] However, the MWCNTs have lower cytotoxicity and therefore are more friendly to the environment.[7]

Several toxicity mechanisms have been proposed for CNTs' antimicrobial activity. These mechanisms include cell membrane perturbation, direct oxidation of cellular

components, and secondary oxidation of cellular lipid bilayer by reactive oxygen species.[8-11]

The functionalized products of CNTs area less-toxic alternative for both in vitro and in vivo.[12,13] Covalent functionalizations[14-19] and non-covalent functionalizations of the CNTs[20-22] are two main approaches to extend the range of their potential applications. Covalent functionalizations include the oxidation of the defective carbon atoms by strong oxidants on the sidewall or at the end of CNTs to generate carboxylic acid groups or carboxylated fractions, which can be chemically modified *via* amidation or esterification. Various polymers,[18] metals[23,24] and biological molecules[25-27] can be grafted to the surface of carboxylated CNTs. While the non-covalent functionalization involves the adsorption of the modified molecules onto the outer surface of the CNTs, the adsorption is carried out by 1) hydrophobic interactions, 2) π–π interactions, 3) electrostatic interactions between ionic adsorbates.[28-30]

In particular, CNTs-based nanomaterials have revealed efficacious bactericidal properties against different pathogenic microorganisms. Previous results exhibited that the modification of MWCNTs with dapsone drug demonstrated significant antibacterial activity than oxidized MWCNTs.[31] In another study, Zhu et al.[31] deposited carbon nanotubes/chitosan composites onto Ti surface via electrophoretic deposition. Subsequently, the Ti surface was coated with different contents of ZnO via atomic layer deposition. The results showed that this coating enhanced the medical implants against *Escherichia coli* (EC) of over 73% and *Staphylococcus aureus* (SA) of over 98%.[32] Another study by Mocan et al revealed that the covalent functionalization of MWCNTs with different concentrations of immunoglobulin G enhanced the apoptosis rates of the immunoglobulin G-MWCNTs against (SA) compared to nonfunctionalized MWCNTs.[33] More recently, Wenyi Wang et al have examined the effect of sodium lignosulfonate-CNT/hybrid polyethersulfone ultrafiltration membranes on bacterial properties with and without applying a weak electric field. Results showed that all the fabricated membranes did not affect bacteria without applying an electric field, the antibacterial influence was only achieved by using an electric field. In conclusion, the application of electric field showed significant antibacterial properties for the prepared membranes.[34]

On the other hand, the ring of pyrazole is essential for biological activity because it is a fertile template for medicinal agents such as antibacterial,[35] antifungal,[36]
anti-inflammatory,[37] analgesic,[38] and others. Moreover, pyrazole derivatives have been the building block for various drugs. For example, rimonabant serves as a cannabinoid receptor and is used to treat obesity and fomepizole inhibits alcohol dehydrogenase. Some of the pyrazole derivatives have significant applications in material liquid crystals[39] and electroluminescence[40] properties. Besides, pyrazole rings not only used as synthetic reagents in multicomponent reactions[41] and chiral auxiliaries,[42] butit is also used as extraction reagents for many metal ions.[43] In addition, some different companies successfully developed many pyrazole derivatives. These derivatives are used in various fields such as chlorantraniliproleas insecticides, pyraclostrobin as fungicides and antipyrine which is used in medicinal chemistry.

The heterocyclic compounds with amide groups are exhibiting extensive biological activities, such as herbicidal,[44,45] anticancer,[46] plant growth regulation[47] and others. Recently, benzovindiflupyr and sedaxane fungicides had been introduced for the treatment of fruit and vegetable crops.

In this work, some pyrazole derivatives were grafted on the surface of the MWCNTs *via* diazonium salts. The prepared samples were characterized by Fourier transform infrared (FTIR) spectroscopy, transmission electron microscopy (TEM), X-ray diffraction and thermogravimetric (TGA) analysis. The synthesized compounds were investigated against three various bacteria (*Staphylococcus Aureus, Bacillus subtilus* and *Escherichia coli*) and two fungal (*Candida Albicans* and *Aspergillusniger*). Also, the molecular docking study was used to examine the binding mode of the pyrazole derivatives inside the binding site of Farnesyl pyrophosphate synthase (FPPS) which represents the efficient target of antimicrobial chemotherapy.[48]

Experimental
Materials and solvents
Concentrated sulfuric acid (H_2SO_4), concentrated nitric acid (HNO_3), sodium nitrite ($NaNO_2$), ethanol and *N,N*-dimethylformamide (DMF) are obtained from Sigma Chemical Company. All other reagents and solvents were purchased from Aldrich and used as received without purification.

Staphylococcus aureus (SA,ATCC 29213), *Bacillus subtilus* (*BS*, RCMB 010067) as gram-positive bacteria and *Escherichia coli* (*EC*, RCMB 010052) as Gram-negative bacterium and *Candida Albicans* (CA, ATCC 10231) and *Aspergillusniger* (*AS*, ATCC16404) as fungi, were

provided by the regional center for mycology and biotechnology, Azhar University, Egypt.

Synthesis of 2-arylazomalononitriles (B)

2-Arylazomalononitriles (**B**) were prepared according to the method described previously[49] as shown in (Scheme 1). As a general route, aromatic amines (**A**) (10 mmol) were dissolved in 10 ml of 33% HCl with stirring and cooled in an ice-salt bath to 0 °C. A cold sodium nitrite solution (10 mmol) was dropwise added with stirring at temperature 2–5 °C to the resulting solution. After completing the addition, the cold mixture was dropwise added to an ice-cold solution of malononitrile (10 mmol) in 10 ml of ethanol with 0.5 gm of sodium acetate. The reaction mixture was further stirred at 0–5 °C for 2 h, and then the precipitated product was filtered. Lastly, the final product was washed with water, and then recrystallized from ethanol.

## Synthesis 4-arylazo-3,5-diamino-1-phenylpyrazoles 1a-c

A mixture of 2-arylazomalononitriles **B** (3 mmol) and phenylhydrazine (0.5 g, 3 mmol) in 30 ml ethanol was refluxed for 6 h with continuous stirring (Scheme 1). The formed solid was filtered off and recrystallized from absolute ethanol.[50]

1-Phenyl-4-(phenyldiazenyl)-1*H*-pyrazole-3,5-diamine (**1a**)

Orange crystals, yield 90%, m.p 175 °C [176 °C],[50] IR (KBr, cm^{-1})ν: 3428 (N-H), 2930 (=CH), 1620 (C=C), 3050 (Ar-CH). Anal.calcd for $C_{15}H_{14}N_6$ (278.32): C, 64.73; H, 5.07; N, 30.20. Found: C, 64.88; H, 5.18; N, 30.40.

4-[(4-Nitrophenyl)diazenyl]-1-phenyl-1*H*-pyrazole-3,5-diamine (**1b**)

Yellow crystals, yield 85%, m.p 165 °C[166 °C],[50] IR (KBr, cm^{-1})ν: 3423 (N-H), 2940 (=CH), 1608 (C=C),
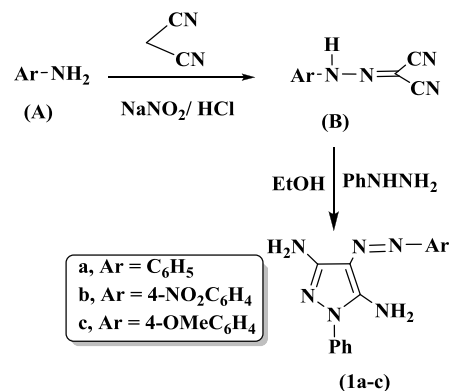
**Scheme 1** Synthesis of 4-phenyldiazenyl-1*H*-pyrazole-3,5-diamine **1a-c**.

1558 (NO$_2$), (Ar-CH). Anal.calcd for $C_{15}H_{13}N_7O_2$ (323.32): C, 55.72; H, 4.05; N, 30.33. Found: C, 55.87; H, 4.22; N, 30.54.

4-[(4-Methoxyphenyl]diazenyl)-1-phenyl-1*H*-pyrazole-3,5-diamine (**1c**)

Brown crystals, yield 92%, m.p 185 °C[186 °C],[50]IR (KBr, cm^{-1})ν: 3428 (N-H), 2930 (=CH), 1620 (C=C), 1246 (O-CH$_3$), (Ar-CH). Anal.calcd for $C_{16}H_{16}N_6O$ (308.34): C, 62.32; H, 5.23; N, 27.26. Found: C, 62.49; H, 5.39; N, 27.45.

Synthesis of ethyl-2-cyano-3-(substituted) phenylacrylates (C)

Ethylcyanoacetate (5mmol) in 10 ml ethanol was dropwise added to the appropriate aldehyde (5mmol) (benzaldehyde, 4-methoxybenzaldehyde and 4-chlorobenzaldehyde) in the presence of few drops of piperidine (Scheme 2). The reaction mixture was stirred for 4–6 h at room temperature. The obtained solidwas then filtered off and washed with cold water. Subsequently, the obtained product was recrystallized from ethanol. The product was TLC pure and gave melting temperatures as reported previously.[51]
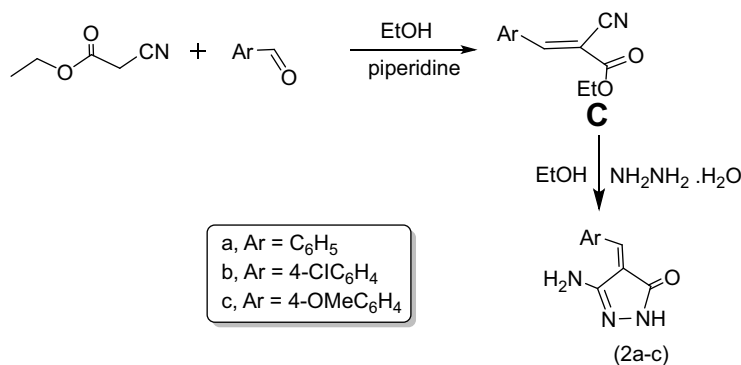
Scheme 2 Synthesis of 5-amino-4-benzylidene-2,4-dihydro-3*H*-pyrazol-3-ones **2a-c**.

Synthesis of 5-amino-4-benzylidene-2,4-dihydro-3*H*-pyrazol-3-one (2a-c)

A mixture of ethyl-2-cyano-3-phenylacrylate (**C**) (10mmol) and hydrazine hydrate (20 mmol) in the presence of ethanol (6 ml) was heated under reflux for 3 h (Scheme 2); then cooled up to the room temperature. Subsequently, the solid products were separated upon dilution of cooled water and filtered off, washed several times by distilled water and dried. The obtained products were recrystallized from ethanol.[51]

3-Amino-4-[(phenyl)methylene]-1*H*-pyrazol-5(4*H*)-one (**2a**)

Yellow crystals, yield 68%, m.p 109 °C [108 °C],[51] IR (KBr, cm^{-1})ν: 3428 (N-H), 2930 (=CH), 1682 (C=O), 1620 (C=C). Anal. calcd for $C_{10}H_9N_3O$ (187.20): C, 64.16; H, 4.85; N, 22.45. Found: C, 64.34; H, 4.70; N, 22.65%.

3-Amino-4-[(4-chlorophenyl)methylene]-1*H*-pyrazol-5(4*H*)-one (**2b**)

Yellow crystals, yield 70%, m.p 97 °C [98 °C],[51] IR (KBr, cm^{-1})ν: 3209 (N-H), 2940 (=CH), 1683 (C=O), 1619 (C=C), 780 (C-Cl). Anal. calcd for $C_{10}H_8N_3OCl$ (221.64): C, 54.19; H, 3.64; Cl, 15.99; N, 18.96. Found: C, 54.37; H, 3.80; Cl, 15.84; N, 18.77%.

3-Amino-4-[(4-methoxyphenyl)methylene]-1*H*-pyrazol-5(4*H*)-one (**2c**)

Yellow crystals, yield 65%, m.p 99 °C[100 °C],[51] IR (KBr, cm^{-1})ν: 3361 (N-H), 2959

(=CH), 1620 (C=O), 1612 (C=C), 1355 (CH$_3$). Anal. calcd for $C_{11}H_{11}N_3O_2$ (217.23): C,

60.82; H, 5.10; N, 19.34. Found: C, 60.63; H, 5.27; N, 19.41%.

Synthesis and oxidation of MWCNTS

MWCNTs were produced via the chemical vapor deposition (CVD) method, as reported previously.[52] Acetylene and Fe/Al$_2$O$_3$ were used as precursor and catalyst, respectively. The MWCNTs were washed with concentrated HCl to remove the catalyst and its support and then were purified with concentrated HNO$_3$ to remove the amorphous carbon particles.

To produce MWCNTs-COOH, (1.0 g) from the neat MWCNTs were sonicated with a 80 ml mixture of HNO$_3$ and H$_2$SO$_4$ (3:1) for 24 h at 90 °C. The reaction mixture was diluted in 250 ml of distilled water, after cooling, and then vacuum-filtered through a 3 μm porosity filter paper. Subsequently, the obtained product was washed several times by distilled water until the pH of the filtrate was 7.0. The obtained product was dried under vacuum oven at 60 °C for 24 h.

Grafting of 4-arylazo-3,5-diamino-1-phenylpyrazoles and 5-amino-4-benzylidene-2,4-dihydro-3*H*-pyrazol-3-one onto MWCNTs-COOH

Either 4-phenyldiazenyl-1*H*-pyrazole-3,5-diamine (**1a-c**) or 5-amino-4 benzylidene-2,4-dihydro-3*H*-pyrazol-3-one (**2a-c**) (4.2 mmol) were mixed with MWCNTs-COOH (100 mg) and NaNO$_2$ (290 mg, 4.2 mmol) then concentrated H$_2$SO$_4$ (0.18 ml, 3.4 mmol) was then added. The mixture was sonicated and heated for 1 h at 60 °C (Scheme 3). After cooling the reaction to room temperature, DMF was added, and the solid was filtered. The solid product was sonicated in DMF many times to remove any unreacted aminopyrazole derivatives from the final product. The sample was then dried at 60 °C in a vacuum oven for 24 h. The general route of the synthesis is outlined in (Scheme 3).

The obtained compounds, MWCNTs-COOH and grafted MWCNTs-COOH, are abbreviated here as CNTs, CNTs-1a, CNTs-1b, CNTs-1c, CNTs-2a, CNTs–2b, and CNTs-2c.

Characterization

The FTIR spectra were recorded on a Perkin Elmer 2000 spectrophotometer in the range of 400–4000 cm^{-1} using KBr pellets. All measurements were carried out with 64 scans at a resolution of 2 cm^{-1} at room temperature.

The morphology of the functionalized MWCNTs was examined by a field emission scanning electron microscope (FE-SEM)(LEO SUPRA 55, Carl Zeiss, Germany) and a transmission electron microscopy (TEM, LEO 912 AB electron microscope). The samples for FE-SEM analysis were prepared by taking one drop of acetone containing the dispersed MWCNTs on a silicon wafer and allowing it to dry in a vacuum oven for 30 min. For TEM, the samples were sonicated in ethanol for 10 min, and few drops of suspension were spread onto a silicon substrate and allowed to evaporate to dryness.

X-ray diffractograms (XRD) of the tested samples were obtained using an X-ray powder diffractometer (a
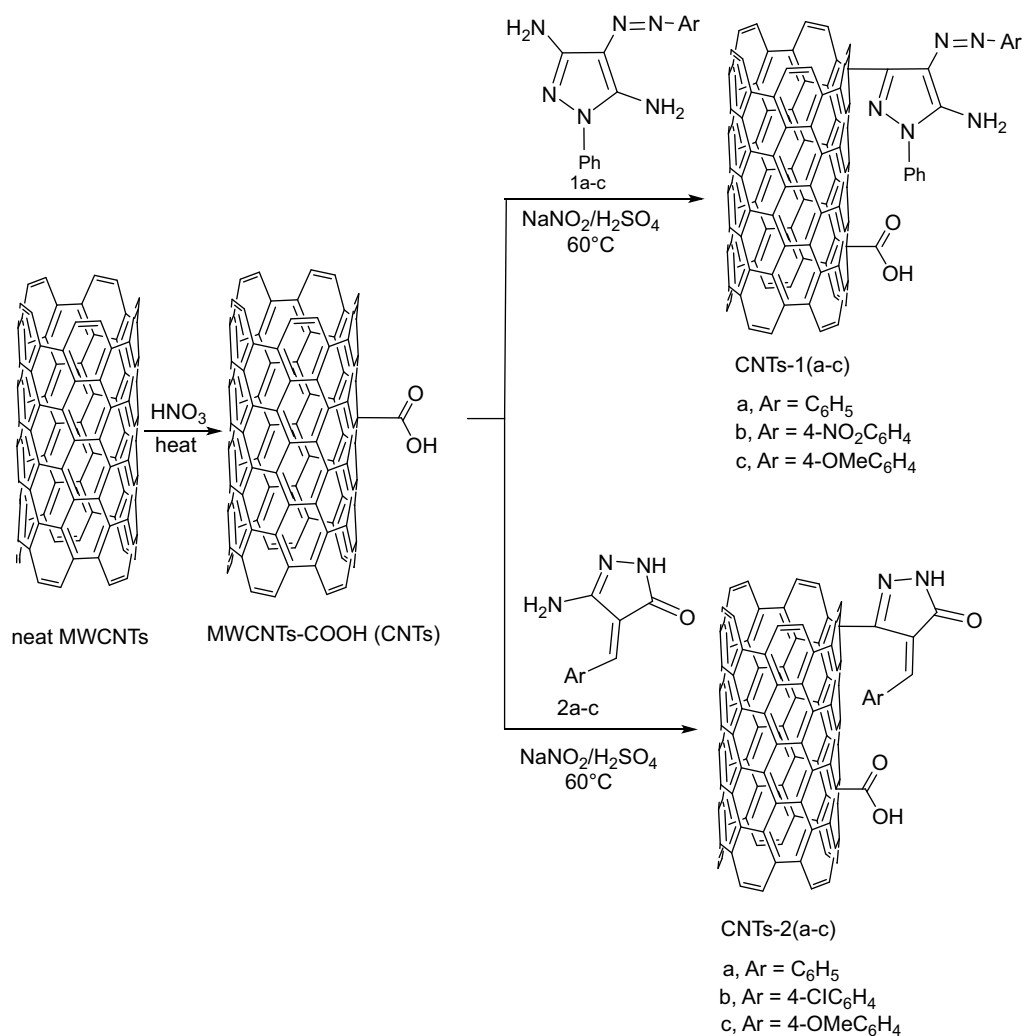
Scheme 3 Grafting of 4-phenyldiazenyl-1*H*-pyrazole-3,5-diamine, **1(a-c)**, and 5-amino-4-benzylidene-2,4-dihydro-3*H*-pyrazol-3-one, **2(a-c)**, onto MWCNTs-COOH.

Philips Xpert MPD Pro) with Ni-filter and Cu Kα radiation source at an accelerating voltage/current of 50 kV/40 mA. The relative intensity was recorded in the scattering range 2θ, varying from 3 °C to 60 °C at scanning rate 2°/min.

Thermogravematric analysis and their derivatives (TGA and DTAG) curves of the functionalized MWCNTs were conducted using Shimadzu TGA-50 H Thermal Analyzer under nitrogen with a dynamic heating rate of 10 °C/min. All experiments were conducted from room temperature to 800 °C, and the reference material was alumina. The sample weights in all experiments were taken around 2.0 mg.

Zeta potential measurements were carried out using Malvern Zetasizer Nano ZS (UK). The measurements were performed at a temperature of 25 °C in triplicate. Samples were sonicated in distilled water and appropriately diluted prior to measurement.

Biological activity

The synthesized pyrazole, pyrazolone derivatives and the grafted MWCNTs were tested against two Gram-positive bacteria (*SA*,ATCC 29213), (*BS*, RCMB 010067),(*EC*, RCMB 010052), as Gram-negative bacterium, and (CA, ATCC 10231) and (*AS*, ATCC 16404), as fungi using Sabouraud Dextrose Agar medium. Ampicillin, gentamicin and amphotericin B were used as standard drugs for Gram-positive, Gram-negative, and antifungal activity, respectively. In brief, 5 mL of the sterilized media (prepared by dissolving 10g tryptone, 5 g yeast extract and 10 g sodium chloride in 1000 mL deionizedwater) were poured onto the sterilized Petri dishes (20–25 mL, each Petri dish) and allowed to solidify. In the solidified media, wells (of 6 mm in diameter) were made in the agar medium by using a sterile steel borer. A sterile swab was applied to spread microbial suspension over the surface

of solidified media evenly, and 0.1 mL of dispersed modified MWCNTs suspensions (0.1 mg/ml) was added to each well with the help of micropipette. The plates were incubated at 37 °C for 24 h in case of antibacterial activity and 48 h at 25 °C for antifungal activity. A blank without the tested materials was prepared for comparison. Zones of inhibition were estimated by measuring the diameter of the bacterial or fungal growth inhibition zone. The values were averaged from three independent experiments (Table 1).

S. aureus was chosen to evaluate the quantitative test of antibacterial activity of the grafted CNTs using spread agar-plating method and cultured with a Luria-Bertani (LB) culture medium according to the method reported previously.[53] Different samples were placed into a 96-well plate, and 200 μl of the suspension of each sample (0.1 mg/ml) was added to approximately 10^7 CFU·ml^{-1} colony of bacteria, then was inoculated with LB culture medium (pH 7.4) at 37 °C for 24 h. The bacterial colony on the plates was observed by a digital camera, and the number of colonies was counted. The antibacterial efficacy was calculated as follows:

$$Antibacterial\ efficacy(\%) = \frac{\begin{pmatrix} Number\ of\ CFUs \\ in\ control\ group \\ -Number\ of\ CFUs \\ in\ experimtal\ group \end{pmatrix}}{\begin{array}{c} Number\ of\ CFUs \\ in\ control\ group \end{array}} \times 100$$

Molecular docking study

Docking was carried out using MOE 2009.10 software, the 3D crystal structure of farnesyl pyrophosphate synthase (FPPS) then saved as Moe file. The 2D structure of docked compounds **1c, 2a, 1b**, CNTs-**1c** CNTs-**2a** and CNTs-**2b** was converted into 3D structures, and energy minimization was carried out then saved as mol. The docking energy was recorded for the selected compound interaction with epidermal growth factor receptor protein (Table 2).

Results and discussion
FTIR

The FTIR spectra of CNTs, CNTs-(**1a-c**) and CNTs-(**2a-c**) are shown in Figure 1 and Figure 2, respectively. The oxidized MWCNTs, sample CNTs, showed peaks at 1747, 1024, 3422,

Table 1 Antimicrobial activity of the synthesized pyrazole, **1(a-c)**, and pyrazolone, **2(a-c)** derivatives and grafted CNTs, CNTs-**1(a-c)** and CNTs-**2(a-c)**.

Samples code	Gram positive bacteria		Gram negative bacteria	Fungi	
	Staphylococcus aureus (SA)	*Bacillus subtilis (BS)*	*Escherichia coli (EC)*	*Aspergillusniger (AS)*	*Candida albicans (CA)*
1a	8	11	NA	NA	9
CNTs-**1a**	NA	NA	NA	NA	NA
1b	NA	NA	NA	NA	11
CNTs-**1b**	9	NA	19	NA	16
1c	14	8	NA	NA	11
CNTs-**1c**	23	9	18	NA	18
2a	11	8	NA	NA	12
CNTs-**2a**	12	8	13	6	12
2b	NA	10	8	NA	10
CNTs-**2b**	12	20	12	7	NA
2c	14	9	8	NA	NA
CNTs-**2c**	14	9	8	NA	NA
CNTs	NA	NA	NA	NA	NA
Trimethoprim/ sulphamethoxazole	20	21	19	26	18
Chloramphenicol	30	24	29	29	25
DMSO	NA	NA	NA	NA	NA

Abbreviations: CNTs, carbon nanotubes; DMSO, dimethyl sulfoxide; NA, not detected.

Table 2 The results obtained from docking study of **1c, 2b**, CNTs-**1c** and CNTs-**2b** using MOE 2009 software

Sample code	Docking energy kcal/mol	Amino acids residue involved in docking interaction	No of hydrogen bond	Length of hydrogen bonds Å
1c	−9.0211	Thr181	2	3.52 Å H-acceptor
		Ser113		1.91 Å H-acceptor
2b	−6.5027	Thr181	1	2.15 Å H-acceptor
CNTs-**1c**	−32.2912	Tyr 218	3	2.54 Å H-acceptor
		Lys 214		2.47 Å H-acceptor
		Arg 74		1.84 Å H-acceptor
CNTs-**2b**	−25.3870	Lys 214	2	2.09 Å H-acceptor
		Gln 254		1.87 Å H-acceptor

Abbreviation: CNTs, carbon nanotubes.
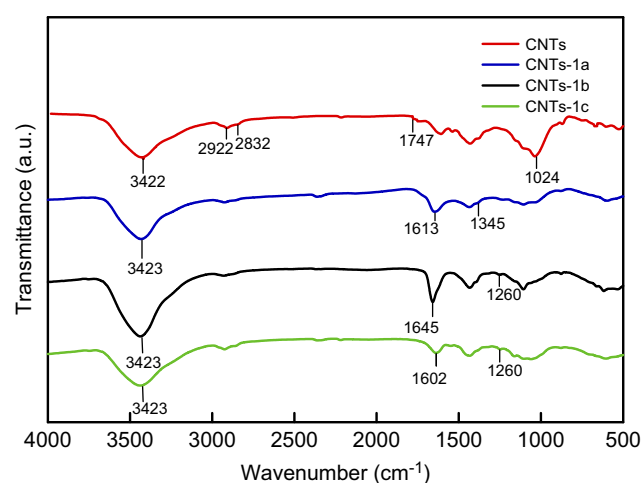
Figure 1 FTIR spectra of CNTs and CNTs-**1(a-c)**.
Abbreviations: CNTs, carbon nanotubes; FTIR, Fourier transform infrared spectroscopy.
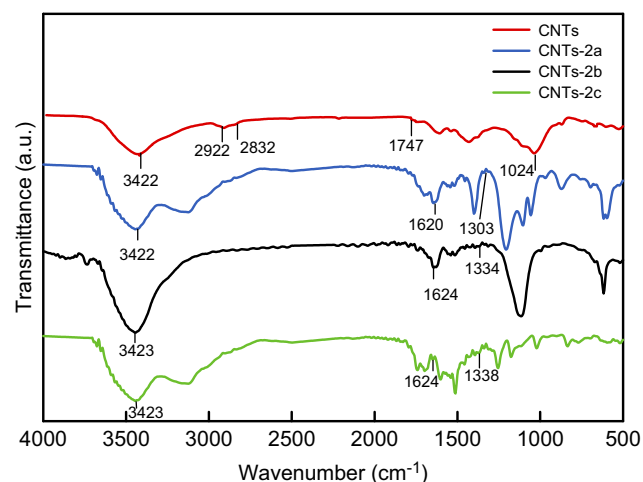
Figure 2 FTIR spectra of CNTs and CNTs-**2(a-c)**.
Abbreviations: CNTs, carbon nanotubes; FTIR, Fourier transform infrared spectroscopy.

2832 and 2922 cm^{-1} which can be assigned to C=O stretching C–O, OH stretching of the carboxylic acid group, asymmetric and symmetric H-C stretching of H-C=O in the carboxyl group, respectively,[54] formed on the side wall of the MWCNTs. The above results propose that MWCNTs have been oxidized successfully. As can be seen from Figures 1 and 2, new peaks appeared in the spectra of CNTs-(**1a-c)** and CNTs-(**2a-c)** at 1260–1345 cm^{-1}, 1602–1645, 3100–3500 cm^{-1} are due to C-N bond stretching, N-H in-plane and N-H stretching which overlapped with the OH stretching, respectively.[55] These results indicate that the surface of MWCNTs has been grafted with 3,5-diamine-4-arylazo-pyr-azole as well as an aminopyrazolone moiety.

EDX spectrum

Further evidence for the grafting of the oxidized MWCNTs was provided by energy dispersive X-ray spectroscopy (EDX) analysis.[56,57] A typical EDX spectrum of CNTs grafted with 5-amino-4-benzylidene-2,4-dihydro-3*H*-pyrazol-3-one **2a**. The (CNTs-**2a**) compound is displayed in Figure 3, and the elemental compositions of the elements in a chosen region are listed in Table inserted in Figure 3B. It is evident that the sample contains carbon (C), nitrogen (N) and oxygen (O) elements with atomic percentage ratio of C:N:O (89.49:4.43:4.96) which confirms the oxidation and grafting of CNTs.

TEM microscopy

The surface morphology of CNTs after grafting was observed using TEM. The TEM images of CNTs and grafted CNTs; namely CNTs-**1a** and CNTs-**2a**, as representative examples, are shown in Figure 4. The remaining samples are given in supplementary
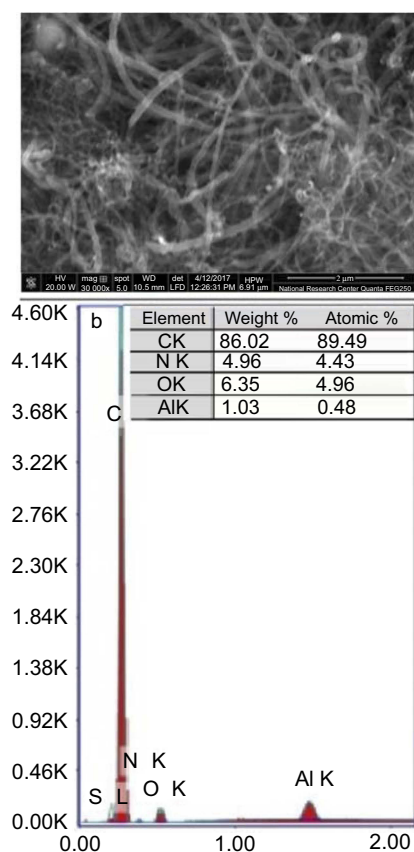
Figure 5 XRD patterns of CNTs and grafted CNTs with pyrazole derivatives, CNTs-1(**a-c**).
Abbreviations: CNTs, carbon nanotubes; XRD, X-ray diffractogram.

Figure 3 (**A**) The selected region of scanning electron microscope (SEM) image of CNTs grafted with 5-amino-4-benzylidene-2,4-dihydro-3*H*-pyrazol-3-one (CNTs-**2a**); (**B**) the corresponding EDX spectrum of CNTs-**2a**.
Abbreviation: CNTs, carbon nanotubes.

information (Figure S1). As shown in Figure 4A, the oxidized MWCNs sample (CNTs) exhibited a lower degree of entanglement because of the presence of carboxyl groups. On the other hand, grafted samples (Figure 4B and 4C) had lower interspaces between nanotubes than oxidized MWCNTs due to the presence of aminopyrazolone moiety. Besides, the tubular structure of the grafted CNTs that observed in the TEM images suggesting the immobilization of the aminopyrazolone moiety onto CNTs surface *via* a covalent
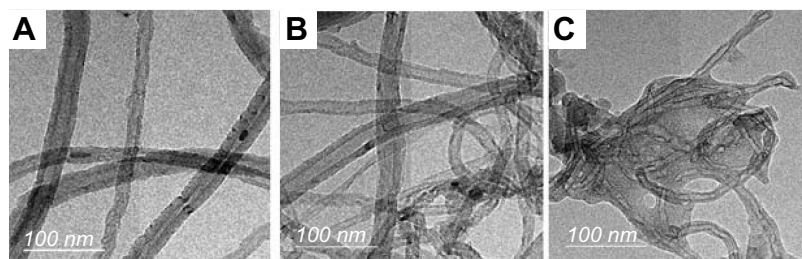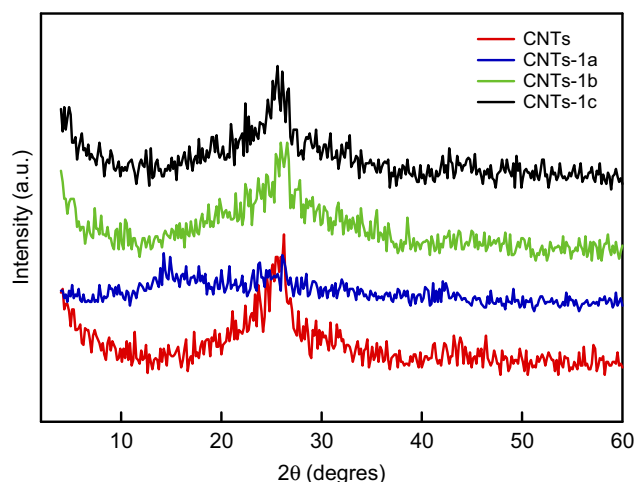
bondwhichdid not deteriorate the structural integrity of MWCNTs.

X-ray diffraction study

Figures 5 and 6 show the XRD pattern of the grafted CNTs (**1a-c**) and CNTs(**2a-c**). For the sake of comparison, these figures included the XRD spectrum of CNTs. The XRD patterns of the oxidized MWCNTs (CNTs) revealed the presence of two peaks at 26.40° and 43.33°, corresponding to (002) and (100) planes of the carbon atoms, respectively.[58] Interestingly, it is obvious that there is no pronounced shift in the position of characteristic peaks of grafted CNTs(**1b**) and CNTs(**1c**) samples compared with CNTs, suggesting that MWCNTs are kept with their original structure after grafting. In contrast, the diffraction peaks around 26.40° and 43.33° are almost disappeared in the spectra of the sample CNTs(**1a**), indicating that the CNTs(**1a**) exhibits lower crystallinity compared with CNTs(**1b**) and CNTs(**1c**) samples. For CNTs(**2a**), the

Figure 4 TEM micrographs of (**A**) CNTs, (**B**) CNTs-**1a**and (**C**) CNTs-**2a**.
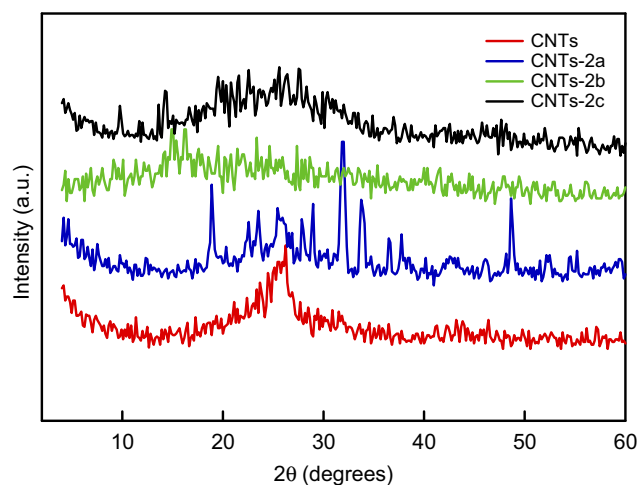**Abbreviations:** CNTs, carbon nanotubes; TEM, transmission electron microscopy.

Figure 6 XRD patterns of CNTs and grafted CNTs with pyrazolone derivaties, CNTs-2(**a-c**).
Abbreviations: CNTs, carbon nanotubes; XRD, X-ray diffractogram.

peak in the vicinity of 26.40° was weakened, and the one at 43.33° became broader and high intensity. In addition, other peaks are observed around 19.04°and 31.97°. For sample CNTs(**2b**), the diffraction peaks around 26.40°, and 43.33° are almost disappeared. In the spectra of the sample CNTs(**2c**), the diffraction peaks around 26.40° became broader. This indicates that CNTs(**2b**) processes lower crystallinity compared with **CNTs(2a)** and **CNTs(2c)**.

Thermogravimetric analysis

The thermogravematric analysis (TGA) provide a quantitative evaluation of the extent of grafting. Figures 7 and 8 show the TGA thermograms and their derivatives (DTGA) of the CNTs and CNTs grafted samples. As can be seen, CNTs is thermally stable up to 550 °C. For CNTs grafted with the pyrazole as well as pyrazolone derivatives, all the the rmograms, except CNTs-**2a**, exhibit three steps of weight losses. The first one ends below 120 °C is related to the evaporation of the moisture water. This step is followed by a significant degradation step which occurs between 120–410 °C. This weight loss step is probably due to the decomposition of the grafted pyrazole as well as pyrazolone derivatives and carboxylic functional groups on the CNTs surface. The weight losses are found to be 7.1, 24.1, 16.9, 16.3, 22.0, 14.4 and 14.2% for CNTs, CTNs-**1a** CNTs-**1b**, CNT-**1c**, CNT-**2a**, CNTs-**2b** and CNTs-**2c**, respectively. The weight difference between the CNTs and grafted samples can be attributed to the introduction of the grafted pyrazole as well as pyrazolone onto the surfaces of CNTs. The difference in the percentage of weight losses is probably due to the difference in the
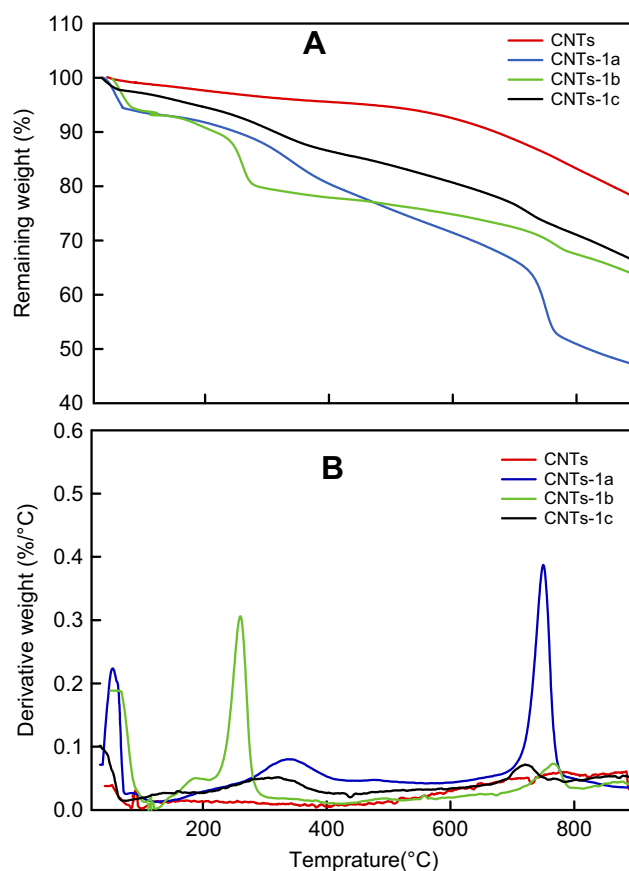

Figure 7 TGA (**A**) and DTGA (**B**) curves of CNTs, CNTs(**1a**), CNTs(**1b**) and CNTs(**1c**).
Abbreviations: CNTs, carbon nanotubes; DTGA, derivative of thermogravematric analysis; TGA, thermogravematric analysis.

molecular weight of the grafted pyrazole as well as pyrazolone derivatives and their reactivity toward reaction with CNTs.

Biological activity

The synthesized pyrazoles (**1a-c**), pyrazolone derivatives (**2a-c**) and CNTs grafted samples were evaluated for their in vitro antibacterial activity against (SA) and (BS) as examples of Gram-positive bacteria and (EC) as examples of Gram-negative bacteria. The investigated samples were also evaluated for their in vitro antifungal potential against a representative panel of fungal strains such as (AS) and (CA). The sensitivity of the tested organisms was assayed against the action of suspension solutions (at 1 mg/mL concentration) using inhibition zone diameter in mm as a criterion for the antimicrobial activity (agar well diffusion method). As shown from the results listed in Table 1, the synthesized compounds **1a-c**, CNTs(**1a-c**), **2a-c** and CNTs(**2a-c**) showed no antifungal activity in vitro against fungus (AS) under the screening conditions except the
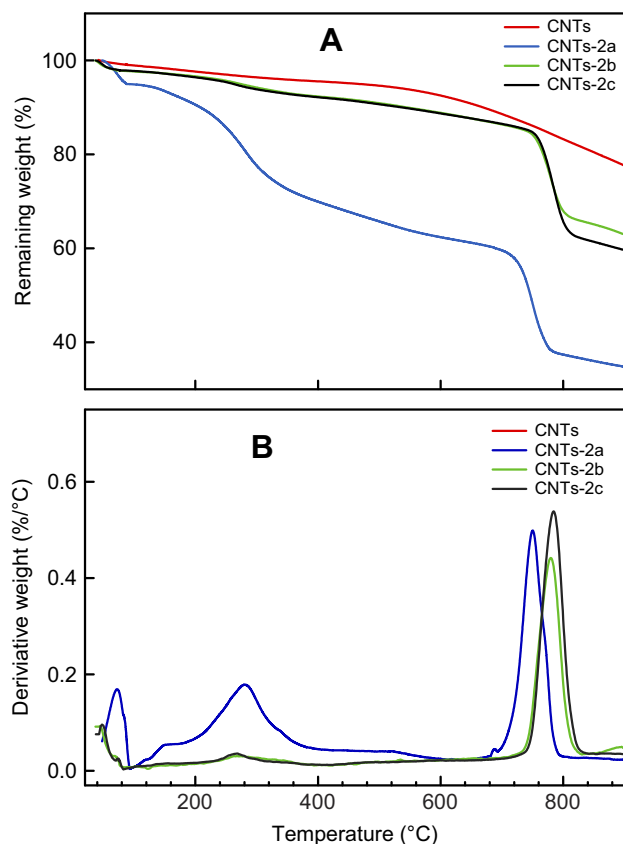
Figure 8 TGA (**A**) and DTGA (**B**) curves of CNTs, CNTs(**2a**), CNTs(**2b**) and CNTs(**2c**).
Abbreviations: CNTs, carbon nanotubes; DTGA, thermogravematric analysis; TGA, derivative of thermogravematric analysis.

compounds CNTs(**2a,b**) showed weak activity. On the other hand, compound CNTs(**1c**) showed activity against the pathogenic yeast (CA) well as a reference drug trimethoprim/sulphamethoxazole. The order of the activity against the filamentous fungus yeast (CA) as the following CNTs(**1c**) >CNTs(**1b**)>**2a**>CNTs(**2a**)>**1c** >**1b**>**2b** >**1a**. However, it can be seen that compound CNTs(**1c**), also showed the highest activity against Gram-positive bacterium (SA) compared to trimethoprim/sulphamethoxazole as reference drugs, followed by compounds **1c, 2c**, CNTs(**2c**), CNTs(**2a**), CNTs(**2b**), **2a**, CNTs(**1b**) and **1a**, respectively. Moreover, compound CNTs(**2b**) showed the highest activity against Gram-positive bacterium (BS), as well as a reference drug followed by compounds **1a, 2b**, CNTs(**1c**), **2c**, CNTs(**2c**), **2a**, CNTs(**2a**) and **1c**. Additionally, the compound CNTs(**1b**) showed a higher activity against (EC) as well as standard reference drugs, followed by compounds CNTs(**1c**), CNTs(**2a**), **2b, 2c** and CNTs(**2c**). Comparison between the biological neat pyrazoles, pyrazolones and their corresponding grafted CNTs revealed that the grafted samples have better antibacterial and antifungal activity except for compound **2c** and its grafted CNTs(**2c**) which

showed the same activity against three types of bacteria (SA), (BS), and (EC). Generally, the antimicrobial activity depends on many factors such as hydrophobic/hydrophilic interactions, interactions between functional groups localized on the surface of CNTs and bacterial cells, the extent of modification of CNTs and dispersion of modified CNTs in the culture medium. Another factor that is an essential role in the microbial balance and resistance to antimicrobials is the charge of the cell surfaces. Zeta potential (ξ) measurements are carried out to examine the charge on the surface of the tested materials. Representative examples are displayed in the supplementary information (Figure S2). The results showed that the surface charge of CNTs was negative, and it changes after grafting with pyrazole and pyrazolone derivatives. The ξ of CNTs was about -60.3 mV while for CTNs(**1a**), CNTs(**1b**), CNTs(**2a**), CNTs(**2b**) and CNTs(**2c**), were found to be -32.6, -36.2, -25.5, -36.0 and -39.8, respectively. Unexpected, CNTs(**1c**) sample exhibited $+29.5$ mV. The data as mentioned earlier suggest that CNTs sample does not affect demonstrated microorganisms, while CNTs grafted with CNTs grated with pyrazole ring bearing methoxy group is more effective compared to other grafted CNTs pyrazole derivatives, except *AS* fungus. For CNTs(**2a**) with unsubstituted pyrazolone moiety, which possessed less negative charge ($\xi = -25.3$ mV), showed a broad spectrum against gram-positive, gram-negative as well as fungi.

Similarly, grafted CNTs with pyrazolone bearing p-chloro ($\xi = -36.0$ mV) atom exhibited antimicrobial activity, except *CA* fungus. For CNTs(**2c**) grafted with pyrazolone bearing *p*-methoxy group ($\xi = -39.8$ mV) had relatively moderate antimicrobial activity towards tested bacteria and had no activity against fungi. These results inferred that the surface charge of investigated samples do not play a dominant rule of interaction with the bacterial membrane to kill microorganisms [references], but there other factors such as functionality of the CNTs surface, the extent of surface grafting of CNTs and dispersive quality, which participate in different ratios, affect the antimicrobial activity.

The antibacterial activities of the prepared grafted CNTs were also analyzed via the spread plate method (CFU). We focused on *S. aureus* as this Gram-positive bacterium is one of the most widespread pathogens which responsible on a wide range of human diseases like skin, bone, joint and respiratory infections, and endovascular disorders. The calculated antibacterial efficacy of CNTs(**1b**), CTNs(**1c**), CNTs(**2a**), CNTs(**2b**) and CNTs(**2c**) were found to be 74.6, 95.2, 17.5, 20.6 and 30.2%. CNTs(**1a**) has no visible difference for the control group. These results are consistent

with the inhibition zone. Similarly, grafted CNTs with pyrazolone bearing p-chloro (ξ = −36.0 mV) atom exhibited antimicrobial activity, except *CA* fungus. For CNTs(**2c**) grafted with pyrazolone bearing *p*-methoxy group (ξ = −39.8 mV) had relatively moderate antimicrobial activity towards tested bacteria and had no activity against fungi. These results inferred that the surface charge of investigated samples does not play a dominant rule of interaction with the bacterial membrane to kill microorganisms,[59–61] but there other factors such as functionality of the CNTs surface, the extent of surface grafting of CNTs and dispersive quality, which participate in different ratios, affect the antimicrobial activity.

The antibacterial activities of the prepared grafted CNTs were also analyzed via the spread plate method (CFU). We focused on *S. aureus* as this Gram-positive bacterium is one of the most widespread pathogens which responsible on a wide range of human diseases like skin, bone, joint and respiratory infections, and endovascular disorders. The calculated antibacterial efficacy of CNTs (**1b**), CTNs(**1c**), CNTs(**2a**), CNTs(**2b**) and CNTs(**2c**) were found to be 74.6, 95.2, 17.5, 20.6 and 30.2%. CNTs(**1a**) has no visible difference for the control group. These results are consistent with the inhibition zone.

Molecular docking study

We performed docking against Farnesyl pyrophosphate synthase (FPPS) which considered as a precursor for the biosynthesis of essential isoprenoids like carotenoids, ubiquinones, dolichols, sterols, among others and also helps in farnesylation and geranylation of proteins. Also, (FPPS) plays a central role in metabolism through the enzymatic generation of FPP. In addition, FPP, initially used for protein prenylation, synthesis of sterols, dolichols, heme *a*, and ubiquinone, is potently inhibited by bisphosphonates.[62–67] Compounds **1c, 2b**, CNTs-**1c** and CNTs-**2b** were docked against (FPPS) to investigate if these compounds have a similar mechanism as (FPPS) inhibitors. The protein used obtained from a protein data bank (pdb, code: 1UBY) saved as Moe file.

Docking study was achieved to explore the binding mode of the most active synthesized pyrazole derivatives **1c, 2b**, CNTs-**1c** and CNTs-**2b** inside the binding cavity of (FPPS) and metal complexes as the potential target for antibacterial and antifungal agents. The binding of the most potent conformer of pyrazole CNTs-**1c** inside the binding pocket of target enzyme illustrated by Figure 12,

while Table 2 point out the molecular docking parameters of compounds **1c, 2b**, CNTs-**1c** and CNTs-**2b**. The binding energy of the generated conformers for the potent discovered pyrazole derivative CNTs-**1c** was −32.2912 kcal/mol for the best conformer compared to the pyrazole derivative **1c** with binding energy −9.0211kcal/mol. The best potent conformer CNTs-**1c** fits the binding pocket residues of the enzyme with three hydrogen bonds. The residues were Tyr218, Lys214 and Arg74, with bond lengths 2.54 Å (11%), 2.47 Å(12%) and 1.84 Å (27%), respectively, as depicted from Table 2, in addition to arene-arene bonds between phenyl, pyrazole and carbon nanotube carbons with Lys214, Arg126, Gln254 and Arg127, respectively.Also, CNTs-**2b** fits the binding pocket residues of the enzyme with two hydrogen bonds. The residues were Lys214 with bond lengths 2.09 Å (29%) and Gln254 with bond length 1.87 Å (17%), respectively, as shown from Table 2. The ligands CNTs-**1c**, and CNTs-**2b** showed more interaction with pocket residues of enzyme 1UBY compared with that of the parent pyrazoles**1c, 2b**, and neat **CNTs** as shown in the Figures 9–13. The results obtained from molecular docking study have matched the results obtained from the antimicrobial activity. Binding of the synthesized compounds with the active site of (FPPS) enzyme may support the postulation that these compounds have the same mechanism of (FPPS).

Conclusion

The surface of the carboxylated multi-walled carbon nanotubes (MWCNTs) was successfully grafted with pyrazole and pyrazolone moieties using diazonium salts of pyrazoles and pyrazolones. The grafted MWCTs were
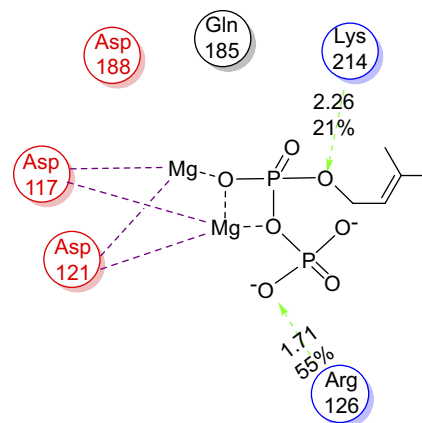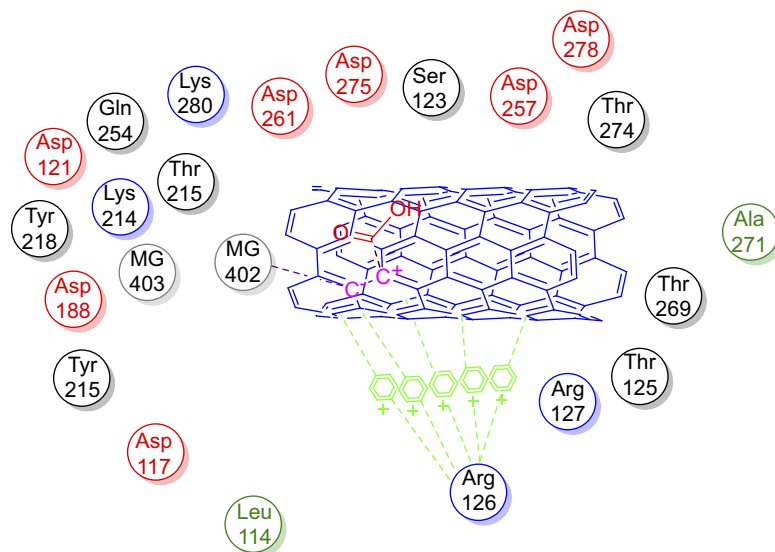

Figure 9 2D the active site of 1UBY.

Figure 10 2D Lignad interaction of neat CNTs with the active site of 1UBY.
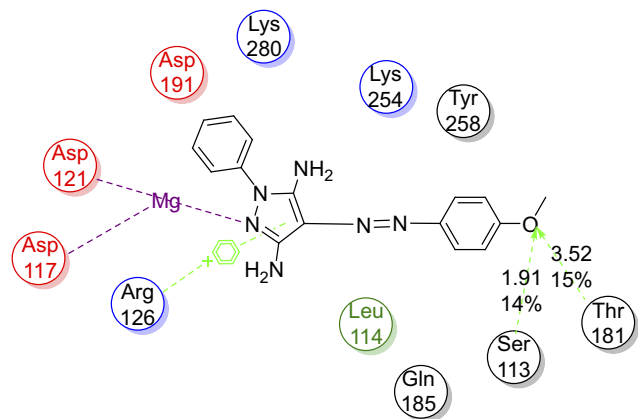**Abbreviation:** CNTs, carbon nanotubes.

Figure 11 2D Lignad interaction of 1c with the active site of 1UBY.

confirmed by FTIR, EDX, TEM, X-ray, and TGA analysis and the results indicated the attachment of pyrazole and pyrazolone moieties onto the surface of the MWCNTs. The study of the biological activity demonstrated that the grafted MWCNTs (samples CNTs-**1b**, CNTs-**1c**, and CNTs-**2a-c**) have significant antibacterial activity against various bacteria (*SA, BS*, and *EC*) and (*CA*) fungus compared with that of neat pyrazole and pyrazolone derivatives. The results of the zeta potential (ξ) vlaues may be inferred that the surface charges of the grafted CNTs and microorganisms did not play the main rule for antimicrobial activity. The functionality of pyrazole and pyrazolone moieties, the extent of grafting and dispersive quality seem
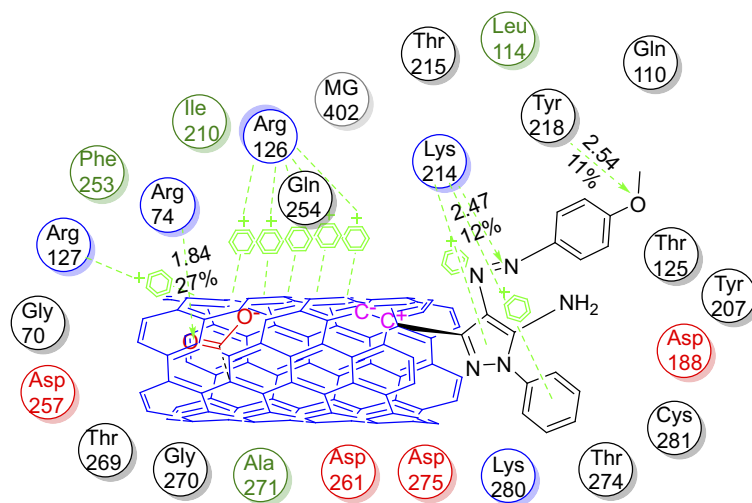

Figure 12 2D Lignad interaction of CNTs-1c with the active site of 1UBY.
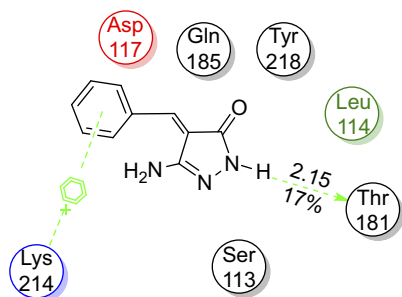**Abbreviation:** CNTs, carbon nanotubes.

Figure 13 2D Ligand interaction of **2b** with the active site of 1UBY.

additional factors that influence the biological activity of the tested materials.

The molecular docking study was performed for the potent pyrazole derivatives and their grafted MWCNTs to show interactions between the most active inhibitors and Farnesyl pyrophosphate synthase (FPPS).

Disclosure

The authors report no conflicts of interest in this work.

References

1. Ajayan PM, Charlier J-C, Rinzler AG. Carbon nanotubes: from macromolecules to nanotechnology. *Proc Natl Acad Sci USA*. 1999;96(25):14199–14200. doi:10.1073/pnas.96.25.14199
2. Lam C-W, James JT, McCluskey R, Arepalli S, Hunter RL. A review of carbon nanotube toxicity and assessment of potential occupational and environmental health risks. *Crit Rev Toxicol*. 2006;36(3):189–217. doi:10.1080/10408440600570233
3. Baughman RH, Zakhidov AA, Wa DH. Carbon nanotubes–the route toward applications. *Science*. 2002;297(5582):787–792. doi:10.1126/science.1060928
4. Lin Y, Taylor S, Li H, et al. Advances toward bioapplications of carbon nanotubes. *J Mater Chem*. 2004;14(4):527–541. doi:10.1039/b314481j
5. Kang S, Pinault M, Pfefferle LD, Elimelech M. Single-walled carbon nanotubes exhibit strong antimicrobial activity. *Langmuir*. 2007;23(17):8670–8673. doi:10.1021/la701067r
6. Kang S, Mauter MS, Elimelech M. Physicochemical determinants of multiwalled carbon nanotube bacterial cytotoxicity. *Environ Sci Technol*. 2008;42(19):7528–7534. doi:10.1021/es8010173
7. Kang S, Herzberg M, Rodrigues DF, Elimelech M. Antibacterial effects of carbon nanotubes. *Size Does Matter! Langmuir*. 2008;24(13):6409–6413. doi:10.1021/la800951v
8. Lyon DY, Fortner JD, Sayes CM, Colvin VL, Hughe JB. Bacterial cell association and antimicrobial activity of a C60 water suspension. *Environ Toxicol Chem*. 2005;24(11):2757–2762. doi:10.1897/04-649R.1
9. Fortner JD, Lyon DY, Sayes CM, et al. C60 in water: nanocrystal formation and microbial response. *Environ Sci Technol*. 2005;39(11):4307–4316. doi:10.1021/es048099n
10. Klaine SJ, Alvarez PJJ, Batley GE, et al. Nanomaterials in the environment: behavior, fate, bioavailability, and effects. *Environ Toxicol Chem*. 2008;27(9):1825–1851. doi:10.1897/08-090.1
11. Li Q, Mahendra S, Lyon DY, et al. Antimicrobial nanomaterials for water disinfection and microbial control: potential applications and implications. *Water Res*. 2008;42(18):4591–4602. doi:10.1016/j.watres.2008.08.015
12. Kang Y, Liu Y-C, Wang Q, Shen J-W, Wu T, Guan W-J. On the spontaneous encapsulation of proteins in carbon nanotubes. *Biomaterials*. 2009;30(14):2807–2815. doi:10.1016/j.biomaterials.2009.01.024
13. Sayes CM, Liang F, Hudson JL, et al. Functionalization density dependence of single-walled carbon nanotubes cytotoxicity in vitro. *Toxicol Lett*. 2006;161(2):135–142. doi:10.1016/j.toxlet.2005.08.011
14. Strano MS, Dyke CA, Usrey ML, et al. Electronic structure control of single-walled carbon nanotube functionalization. *Science*. 2003;301(5639):1519–1522. doi:10.1126/science.1087691
15. Sun Y-P, Fu K, Lin Y, Huang W. Functionalized carbon nanotubes: properties and applications. *Acc Chem Res*. 2002;35(12):1096–1104. doi:10.1021/ar010160v
16. Men X-H, Zhang -Z-Z, Yang J, Wang K, Jiang W. Superhydrophobic/superhydrophilic surfaces from a carbon nanotube based composite coating. *Appl Phys A*. 2010;98(2):275. doi:10.1007/s00339-009-5425-6
17. Zanzan Z, Zhe W, Hulin L. Functional multi-walled carbon nanotube/polyaniline composite films as supports of platinum for formic acid electrooxidation. *Appl Surf Sci*. 2008;254(10):2934–2940. doi:10.1016/j.apsusc.2007.10.033
18. Castro MRS, Lasagni AF, Schmidt HK, Mücklich F. Direct laser interference patterning of multi-walled carbon nanotube-based transparent conductive coatings. *Appl Surf Sci*. 2008;254(18):5874–5878. doi:10.1016/j.apsusc.2008.03.140
19. Chen J, Rao AM, Lyuksyutov S, et al. Dissolution of full-length single-walled carbon nanotubes. *J Phys Chem B*. 2001;105(13):2525–2528. doi:10.1021/jp002596i
20. O'Connell MJ, Boul P, Ericson LM, et al. Reversible water-solubilization of single-walled carbon nanotubes by polymer wrapping. *Chem Phys Lett*. 2001;342(3):265–271. doi:10.1016/S0009-2614(01)00490-0
21. Chattopadhyay D, Lastella S, Kim S, Papadimitrakopoulos F. Length separation of Zwitterion-functionalized single wall carbon nanotubes by GPC. *J Am Chem Soc*. 2002;124(5):728–729. doi:10.1021/ja0172159
22. Chattopadhyay D, Galeska I, Papadimitrakopoulos F. A route for Bulk separation of semiconducting from metallic single-wall carbon nanotubes. *J Am Chem Soc*. 2003;125(11):3370–3375. doi:10.1021/ja0263137
23. Lordi V, Yao N, Wei J. Method for supporting platinum on single-walled carbon nanotubes for a selective hydrogenation catalyst. *Chem Mater*. 2001;13(3):733–737. doi:10.1021/cm000210a
24. Salavati-Niasari M, Bazarganipour M. Covalent functionalization of multi-wall carbon nanotubes (MWNTs) by nickel(II) Schiff-base complex: synthesis, characterization and liquid phase oxidation of phenol with hydrogen peroxide. *Appl Surf Sci*. 2008;255(5):2963–2970. doi:10.1016/j.apsusc.2008.08.100
25. Huang W, Taylor S, Fu K, et al. Attaching proteins to carbon nanotubes via diimide-activated amidation. *Nano Lett*. 2002;2(4):311–314. doi:10.1021/nl010095i
26. Wu Z, Feng W, Feng Y, et al. Preparation and characterization of chitosan-grafted multiwalled carbon nanotubes and their electrochemical properties. *Carbon*. 2007;45(6):1212–1218. doi:10.1016/j.carbon.2007.02.013
27. Zardini HZ, Amiri A, Shanbedi M, Maghrebi M, Baniadam M. Enhanced antibacterial activity of amino acids-functionalized multi walled carbon nanotubes by a simple method. *Colloids Surf B Biointerfaces*. 2012;92:196–202. doi:10.1016/j.colsurfb.2011.11.045
28. Shi B, Zhuang X, Yan X, Lu J, Tang H. Adsorption of atrazine by natural organic matter and surfactant dispersed carbon nanotubes. *J Environ Sci*. 2010;22(8):1195–1202. doi:10.1016/S1001-0742(09)60238-2
29. Pagona G, Tagmatarchis N. Carbon nanotubes: materials for medicinal chemistry and biotechnological applications. *Curr Med Chem*. 2006;13(15):1789–1798. doi:10.2174/092986706777452524
30. Bai Y, Park IS, Lee SJ, et al. Aqueous dispersion of surfactant-modified multiwalled carbon nanotubes and their application as an antibacterial agent. *Carbon*. 2011;49(11):3663–3671. doi:10.1016/j.carbon.2011.05.002

31. Azizian J, Hekmati M, Dadras OG. Functionalization of carboxylated multiwall nanotubes with dapsone derivatives and study of their antibacterial activities against E.coli and S. aureus. *Orient J Chem*. 2014;30(2):667–673. doi:10.13005/ojc

32. Zhu Y, Liu X, Yeung KWK, Chu PK, Wu S. Biofunctionalization of carbon nanotubes/chitosan hybrids on Ti implants by atom layer deposited ZnO nanostructures. *Appl Surf Sci*. 2017;400:14–23. doi:10.1016/j.apsusc.2016.12.158

33. Mocan L, Ilie I, Tabaran FA, et al. Selective laser ablation of methicillin-resistant staphylococcus aureus with IgG functionalized multi-walled carbon nanotubes. *J Biomed Nanotechol*. 2016;12(4):781–788. doi:10.1166/jbn.2016.2221

34. Wang W, Zhu L, Shan B, et al. Preparation and characterization of SLS-CNT/PES ultrafiltration membrane with antifouling and antibacterial properties. *J Membr Sci*. 2018;548:459–469. doi:10.1016/j.memsci.2017.11.046

35. Van Hes R, Wellinga K, Grosscurt AC. 1-Phenylcarbamoyl-2-pyrazolines: a new class of insecticides. 2. Synthesis and insecticidal properties of 3, 5-diphenyl-1-phenylcarbamoyl-2-pyrazolines. *J Agric Food Chem*. 1978;26(4):915–918. doi:10.1021/jf60218a015

36. Lv H-S, Wang L-Y, Ding X-L, Wang X-H, Zhao B-X ZH. Synthesis and antifungal activity of novel (1-arylmethyl-3-aryl-1H-pyrazol-5-yl)(4-arylpiperazin-1-yl)methanone derivatives. *J Chem Res*. 2013;37(8):473–475. doi:10.3184/174751913X13734652599909

37. Garg HG, Prakash C. Potential antidiabetics. 9. Biological activity of some pyrazoles. *J Med Chem*. 1971;14(17):649–650. doi:10.1021/jm00289a028

38. Abd El Razik HA, Badr MH, Atta AH, Mouneir SM, Abu-Serie MM. Benzodioxole-pyrazole hybrids as anti-inflammatory and analgesic agents with COX-1,2/5-LOX inhibition and antioxidant potential. *Arch Pharm (Weinheim)*. 2017;350:5. doi:10.1002/ardp.201700026

39. Kauhanka UM, Kauhanka MM. New metallomesogens with enaminoketonato ligands. *Liq Cryst*. 2006;33(2):213–218. doi:10.1080/02678290500429638

40. Gao X-C, Cao H, Zhang L-Q, Zhang B-W, Cao Y, Huang C-H. Properties of a new pyrazoline derivative and its application in electroluminescence. *J Mater Chem*. 1999;9(5):1077–1080. doi:10.1039/a900276f

41. Tu X-J, Hao W-J, Ye Q, et al. Four-component bicyclization approaches to skeletally diverse pyrazolo[3,4-b]pyridine derivatives. *J Org Chem*. 2014;79(22):11110–11118. doi:10.1021/jo502096t

42. Molteni G, Buttero PD. A bicyclo[3.1.1]heptano[4,3-c]pyrazole derived chiral auxiliary for dipolar cycloadditions. *Tetrahedron Asymmetry*. 2005;16(11):1983–1987. doi:10.1016/j.tetasy.2005.04.014

43. Singh P, Paul K, Holzer W. Synthesis of pyrazole-based hybrid molecules: search for potent multidrug resistance modulators. *Bioorg Med Chem*. 2006;14(14):5061–5071. doi:10.1016/j.bmc.2006.02.046

44. Liu X-H, Weng J-Q, Wang B-L, Li Y-H, Tan C-X, Li Z-M. Microwave-assisted synthesis of novel fluorinated 1,2,4-triazole derivatives, and study of their biological activity. *Res Chem Intermed*. 2014;40(8):2605–2612. doi:10.1007/s11164-013-1113-4

45. Jian-Quan W, Xing-Hai L, Guo-Tong T. Synthesis and herbicidal activity of amide derivatives containing thiazole moiety. *Asian J Chem*. 2013;25(4):2149–2152. doi:10.14233/ajchem.2013.13366

46. Antoszczak M, Maj E, Napiórkowska A, et al. Synthesis, anticancer and antibacterial activity of salinomycin N-benzyl amides. *Molecules*. 2014;19(12):19435–19459. doi:10.3390/molecules190811211

47. Yan S-L, Yang M-Y, Sun Z-H, et al. Synthesis and antifungal activity of 1,2,3-thiadiazole derivatives containing 1,3,4-thiadiazole moiety [Internet]. *Lett Drug Des Discov*. 2014. [cited 2018]. Available from: http://www.eurekaselect.com/121773/article. doi:10.2174/15701808 11666140423222141

48. Bearne SL, Blouin C. Inhibition of Escherichia coli glucosamine-6-phosphate synthase by reactive intermediate analogues. The role of the 2-amino function in catalysis. *J Biol Chem*. 2000;275(1):135–140. doi:10.1074/jbc.275.1.135

49. Elnagdi MH, Sallam MMM, Fahmy HM, Ibrahim SA-M, Elias MAM. Reactions with the arylhydrazones of α-cyanoketones: the structure of 2-arylhydrazono-3-ketimino-nitriles. *Helv Chim Acta*. 1976;59(2):551–557. doi:10.1002/hlca.19760590220

50. Elnagdi MH, Allah SOA. Reactions with the arylhydrazones of some α-cyanoketones. *J Für Prakt Chem*. 1973;315(6):1009–1016. doi:10.1002/prac.19733150604

51. Rajitha G, Prasad KVSRG, Bharathi K. Synthesis and biological evaluation of 3-amino pyrazolones. *Asian J Chem*. 2011;23(2):684–686.

52. Shokry SA, El Morsi AK, Sabaa MS, Mohamed RR, El Sorogy HE. Synthesis and characterization of polyurethane based on hydroxyl terminated polybutadiene and reinforced by carbon nanotubes. *Egypt J Pet*. 2015;24(2):145–154. doi:10.1016/j.ejpe.2015.05.008

53. Xiang Y, Liu X, Mao C, et al. Infection-prevention on Ti implants by controlled drug release from folic acid/ZnO quantum dots sealed titania nanotubes. *Mater Sci Eng C*. 2018;85:214–224. doi:10.1016/j.msec.2017.12.034

54. Zhang J, Zou H, Qing Q, et al. Effect of chemical oxidation on the structure of single-walled carbon nanotubes. *J Phys Chem B*. 2003;107(16):3712–3718. doi:10.1021/jp027500u

55. Ellison MD, Gasda PJ. Functionalization of single-walled carbon nanotubes with 1,4-benzenediamine using a diazonium reaction. *J Phys Chem C*. 2008;112(3):738–740. doi:10.1021/jp076935k

56. Zhao Z, Yang Z, Hu Y, Li J, Fan X. Multiple functionalization of multi-walled carbon nanotubes with carboxyl and amino groups. *Appl Surf Sci*. 2013;276:476–481. doi:10.1016/j.apsusc.2013.03.119

57. Stobinski L, Lesiak B, Kövér L, et al. Multiwall carbon nanotubes purification and oxidation by nitric acid studied by the FTIR and electron spectroscopy methods. *J Alloys Compd*. 2010;501(1):77–84. doi:10.1016/j.jallcom.2010.04.032

58. Lee G-W, Kim J, Yoon J, et al. Structural characterization of carboxylated multi-walled carbon nanotubes. *Thin Solid Films*. 2008;516(17):5781–5784. doi:10.1016/j.tsf.2007.10.071

59. Liu S, Ng AK, Xu R, et al. Antibacterial action of dispersed single-walled carbon nanotubes on Escherichia coli and Bacillus subtilis investigated by atomic force microscopy. *Nanoscale*. 2010;2(12):2744–2750. doi:10.1039/c0nr00441c

60. Ernst WA, Thoma-Uszynski S, Teitelbaum R, et al. Granulysin, a T cell product, kills bacteria by altering membrane permeability. *J Immunol Baltim Md 1950*. 2000;165(12):7102–7108.

61. Vecitis CD, Zodrow KR, Kang S, Elimelech M. Electronic-structure-dependent bacterial cytotoxicity of single-walled carbon nanotubes. *ACS Nano*. 2010;4(9):5471–5479. doi:10.1021/nn101558x

62. Cromartie TH, Fisher KJ, Grossman JN. The discovery of a novel site of action for herbicidal bisphosphonates. *Pestic Biochem Physiol*. 1999;63(2):114–126. doi:10.1006/pest.1999.2397

63. Martin MB, Arnold W, Heath HT 3rd, Urbina JA, Oldfield E. Nitrogen-containing bisphosphonates as carbocation transition state analogs for isoprenoid biosynthesis. *Biochem Biophys Res Commun*. 1999;263(3):754–758. doi:10.1006/bbrc.1999.1404

64. van Beek ER, Löwik CW, Ebetino FH, Papapoulos SE. Binding and antiresorptive properties of heterocycle-containing bisphosphonate analogs: structure-activity relationships. *Bone*. 1998;23(5):437–442. doi:10.1016/S8756-3282(98)00120-3

65. Keller RK, Fliesler SJ. Mechanism of aminobisphosphonate action: characterization of alendronate inhibition of the isoprenoid pathway. *Biochem Biophys Res Commun*. 1999;266(2):560–563. doi:10.1006/bbrc.1999.1846

66. Bergstrom JD, Bostedor RG, Masarachia PJ, Reszka AA, Rodan G. Alendronate is a specific, nanomolar inhibitor of farnesyl diphosphate synthase. *Arch Biochem Biophys*. 2000;373(1):231–241. doi:10.1006/abbi.1999.1502

67. Grove JE, Brown RJ, Watts DJ. The intracellular target for the antiresorptive aminobisphosphonate drugs in dictyostelium discoideum is the enzyme farnesyl diphosphate synthase. *J Bone Miner Res*. 2000;15(5):971–981. doi:10.1359/jbmr.2000.15.9.1798